Computer simulation studies of the growth of strained layers by molecular-beam epitaxy

D. A. Faux
Department of Physics, University of Surrey, Guildford, Surrey GU2 5XH, United Kingdom

G. Gaynor
Department of Chemical Engineering, North Carolina State University, Raleigh, North Carolina 27695-7905

C. L. Carson*
Department of Physics, North Carolina State University, Raleigh, North Carolina 27695-8202

C. K. Hall
Department of Chemical Engineering, North Carolina State University, Raleigh, North Carolina 27695-7905

J. Bernholc
Department of Physics, North Carolina State University, Raleigh, North Carolina 27695-8202
(Received 15 March 1990)

Two new types of discrete-space Monte Carlo computer simulation are presented for the modeling of the early stages of strained-layer growth by molecular-beam epitaxy. The simulations are more economical on computer resources than continuous-space Monte Carlo or molecular dynamics. Each model is applied to the study of growth onto a substrate in two dimensions with use of Lennard-Jones interatomic potentials. Up to seven layers are deposited for a variety of lattice mismatches, temperatures, and growth rates. Both simulations give similar results. At small lattice mismatches ($\lesssim 4\%$) the growth is in registry with the substrate, while at high mismatches ($\gtrsim 6\%$) the growth is incommensurate with the substrate. At intermediate mismatches, a transition from registered to incommensurate growth is observed which commences at the top of the crystal and propagates down to the first layer. Faster growth rates are seen to inhibit this transition. The growth mode is van der Merwe (layer-by-layer) at 2% lattice mismatch, but at larger mismatches Volmer-Weber (island) growth is preferred. The Monte Carlo simulations are assessed in the light of these results and the ease at which they can be extended to three dimensions and to more sophisticated potentials is discussed.

I. INTRODUCTION

Advances in crystal-growth technology during recent years, particularly in the field of molecular-beam epitaxy (MBE), have greatly increased the range and quality of multilayer crystal structures which may be grown.[1-3] MBE permits the close control of the thickness and composition of epitaxial overlayers and therefore allows the fabrication of devices which can be uniquely tailored to specific applications. Of special interest in semiconductor physics is a class of structures which are produced by depositing material onto a substrate which has the same crystal structure as the adsorbate but a slightly different lattice constant. If the deposited layers are sufficiently thin, the adsorbed crystal will grow with the same lattice constant as the substrate; the adsorbate is said to be in registry, or commensurate, with the substrate. The adsorbate is forced to stretch (or compress) in order to maintain the same lattice constant as the substrate, causing a biaxial strain which is accommodated within the adsorbate overlayer. If the deposited overlayer exceeds a certain critical thickness, however, the adsorbate reverts to its preferred lattice constant and a series of misfit dislocations are formed at the interface between the substrate and the adsorbate. The adsorbate is then said to be incommensurate with the substrate. The loss of coherent strain and the presence of high concentrations of dislocations impairs device performance.

Layered semiconductor structures possess unusual electronic properties due to the confinement of the electron density to within the layers. The presence of biaxial strain within the layer, which can be controlled by the appropriate choice of material composition, modifies the band structure and provides increased possibilities for the design of new and improved devices.[4,5] The overlayer thickness that may be grown such that the strain is accommodated entirely within the overlayer depends on a variety of factors, including material type, substrate orientation, temperature characteristics during growth, substrate topology, lattice mismatch, the presence of impurities, and so on. The early stages of the growth process and surface kinetics play a crucial role in determining the ultimate quality of the overlayer. It has been our aim to develop a greater understanding of the early stages of the growth process and to analyze the factors which are likely to affect the ultimate quality of the strained layer.

We have chosen to use the Monte Carlo (MC) computer simulation as the major tool of our study as it allows the properties of a large number of particles to be explored on the basis of a few system-defining assumptions. The vast majority of MC computer simulations of MBE crystal growth performed to date have investigated the growth of a *lattice-matched* crystal onto a substrate using the so-called solid-on-solid (SOS) model.[6-10] Here the adatoms are deposited onto predetermined sites defined by the substrate lattice and make jumps on (and evaporate from) the surface according to a set of prescribed rules. Clarke and co-workers,[9-10] for instance, have successfully reproduced the major features of reflection high-energy electron diffraction (RHEED) measurements for both Si deposited on Si and GaAs deposited on GaAs. This success illustrates the ability of the computer simulation technique to unravel some of the complex features of MBE crystal growth.

The SOS model divides the space into a set of discrete locations which may be occupied by adatoms and employs the MC method to simulate the appropriate surface processes. For *continuous-space* simulations both the MC and molecular-dynamics (MD) method may be used. The first continuous-space computer simulation of epitaxial growth was performed by Schneider *et al.*[11] These authors used a molecular-dynamics technique and assumed that particles interacted via a Lennard-Jones potential. Schneider *et al.*[12] later extended this work to investigate the deposition of silicon on a silicon substrate using an interatomic three-body potential devised by Stillinger and Weber.[13] They observed amorphous-like growth at low temperatures and crystalline growth at high temperatures, in agreement with experiment.

All computer studies described above relate to the more easily implemented problem of lattice-matched crystal growth. The first computer simulation of the growth of an adsorbate whose preferred lattice constant is different from that of the substrate was made by Dodson and Taylor.[14,15] They investigated a system of particles interacting via a Lennard-Jones potential in two dimensions using both continuous-space Monte Carlo[14] and molecular-dynamics techniques.[15] These authors investigated the growth characteristics as a function of mismatch and temperature. Their results provide a useful comparison to the present work. Kobayashi and Das Sarma[16] have employed a discrete-space MC model to study the strained Si/Si-Ge system and, finally, Das Sarma *et al.*[17] have performed molecular-dynamics simulation of epitaxial growth with Lennard-Jones interatomic potentials. They find that growth is preferred for the fcc (111) orientation at about one-half the melting temperature.

The discrete-space and continuous-space simulation techniques each have their strengths and weaknesses. The continuous-space simulations can examine effects which arise due to the small displacements of the atoms from their ideal positions, but these advantages can be offset by the significantly increased amount of computer time required, which, in turn, restricts the variety of phenomena which can be investigated. The discrete-space models are considerably more economical in terms of computer resources and have already proven valuable in the study of lattice-matched systems. For this reason we have opted to use discrete-space simulation methods for the study of strained-layer growth.

We present two new types of discrete-space Monte Carlo simulation techniques for the study of strained-layer growth. The first model, called the interpenetrating-lattice (IL) model, uses a combination of two sublattices. One sublattice would be occupied if the adsorbate grew in perfect registry with the substrate and the second sublattice would be occupied if the adsorbate grew with its preferred lattice constant. The IL model is described in Sec. II B. The second, called the potential-minimum (PM) model, employs a novel method for the discretisation of space and may be considered to be a stage between the IL model and a continuous-space simulation. The adatoms are restricted to the positions of local potential minima which are defined by the nearest-neighbor particle-particle interactions. The sites which may be occupied are defined by the local surroundings and therefore change as the adatoms diffuse from site to site. The PM model is described in Sec. II C.

In the present paper the IL and PM models are applied to a two-dimensional system of particles which interact via a Lennard-Jones potential. This system was also chosen by Dodson and Taylor[14,15] for their continuous-space Monte Carlo and molecular-dynamics simulations. The choice of this system is motivated primarily by its simplicity. It allows us to assess the strengths and weaknesses of the models prior to the extensions to three dimensions and the incorporation of potentials appropriate to semiconductor materials. Finally, there are a number of similarities between the results obtained using this simple system and the behavior of real materials.

The basic parameters and other factors which are common to both the IL and PM models are given in Sec. II A and the descriptions of each computer method are presented in Secs. II B and II C. The results obtained at a variety of lattice mismatches and temperatures are presented in Sec. III. An assessment of the IL and PM models and a discussion of the extension to three dimensions are presented in Sec. IV and the conclusions may be found in Sec. V.

II. MODELS

A. Basic considerations

In this subsection we define the basic parameters used in the simulations and explain the features which are common to both the IL and PM models. The specifics of each model are presented in the following subsections.

The potential energy $U_{ss}(r)$ of a substrate atom due to another substrate atom at a dimensionless distance r is given by the Lennard-Jones form,

$$U_{ss}(r)=\varepsilon(r^{-12}-\alpha_{ss}r^{-6})/\alpha_{ss}^2 , \quad (1)$$

where ε determines the temperature scale and α_{ss} defines the lattice spacing. This potential is truncated at the distance $r=2.71$, where the value of the potential reduces to 1% of its value at the minimum. The equilibrium posi-

tions of the substrate atoms are the sites of a triangular lattice with a lattice spacing of a_s which, for convenience, may be assigned a value of 1 (this sets a scale for the dimensionless distance r). A numerical calculation shows that the minimum lattice energy is obtained for $a_s=1$ if the value of α_{ss} is chosen to be 1.8926. This result means that the nearest neighbors are slightly offset from the minimum in $U_{ss}(r)$, which occurs at $r=1.009\,24$ when $\alpha_{ss}=1.8926$. (Note that if $\alpha_{ss}=2$, the nearest neighbors are at a distance of unity, but this does not provide the lowest-energy configuration if the contributions of all atoms to a distance of 2.71 are included.)

The adsorbate-adsorbate interaction $U_{aa}(r)$ is of the same form as Eq. (1), except that α_{ss} is replaced by α_{aa}, where α_{aa} is given by

$$\alpha_{aa}=\alpha_{ss}/a_a^6 \tag{2}$$

and a_a is the lattice spacing of the adsorbate. An adatom interacts with other adatoms via the potential $U_{aa}(r)$, and with substrate atoms via a potential $U_{sa}(r)$. $U_{sa}(r)$ is assumed to be the average of the potentials $U_{aa}(r)$ and $U_{ss}(r)$. An expression for a_{sa}, the substrate-adsorbate nearest-neighbor distance is easily obtained in terms of α_{aa} and α_{ss} by setting the differential of $U_{sa}(r)$ with respect to r equal to zero. This yields

$$a_{sa}^6=2(\alpha_{aa}^2+\alpha_{ss}^2)/[\alpha_{aa}\alpha_{ss}(\alpha_{aa}+\alpha_{ss})]\ . \tag{3}$$

An important quantity is the lattice mismatch f, which may be defined as

$$f=|a_s/a_a-1|\ . \tag{4}$$

The system is therefore defined by the value of f, which assigns a_a via Eq. (4) (remembering that in these simulations a_s is set equal to 1) and assigns α_{aa} using Eq. (2), and the system temperature in units of kT/ε.

There are some additional features which are common to both the IL and PM models. In both models the substrate atoms are fixed in their ideal positions throughout the simulations. The effect of strain relaxation in the upper layers of the substrate will be confined to a separate study. Periodic boundary conditions operate in the lateral directions, and this is an important factor in determining the size of the simulation cell. The width of the simulation cell must accommodate an integer number of lattice spacings a_a and a_s. Accordingly, at 2%, 4%, 5%, 6%, and 8%, the minimum cell size is $50a_s$ $(=49a_a)$, $50a_s$ $(=48a_a)$, $40a_s$ $(=38a_a)$, $50a_s$ $(=47a_a)$, and $50a_s$ $(=46a_a)$, respectively. In all simulations we have assumed that a_a is larger than a_s.

In both the IL and PM models an atom may jump to an adjacent site located within a certain specified distance which, in all simulations, is fixed at a value 10% larger than a_a. The proposed hop is accepted or rejected according to standard Metropolis MC procedures;[18] that is, if the initial and final configurations have energies E_i and E_f, respectively, the new configuration is accepted if $R<\exp[(E_i-E_f)/kT]$, where R is a random number between 0 and 1. The correct MC algorithm for surface diffusion explicitly includes the energy difference between the *barrier* and the site rather than the difference between the energies of the initial and target sites.[19] This is only practical, however, if the barrier energy is readily calculated and, in any case, an adatom may take a curved path towards the target site, which would complicate the calculation still further. We therefore do not include the effect of barrier heights in the present simulations.

B. Interpenetrating-lattice model

In the IL model the adatoms may only occupy the sites of two interpenetrating triangular sublattices. The two sublattices are referred to as the substrate and adsorbate sublattices and are illustrated in Fig. 1. The lattice constant of the substrate sublattice is equal to a_s, and would be occupied if the deposited crystal grew in perfect registry with the substrate. The height of the first layer above the substrate, h_s, and the spacing between layers, d_s, are chosen so as to ensure that the adatoms occupy the lowest-energy positions. Thus d_s is defined such that the adatom-adatom spacing between layers is equal to a_a, and hence $d_s=(a_a^2-a_s^2/4)^{1/2}$. The value of h_s is determined by numerically evaluating the average energy of a complete first layer of adatoms as a function of the height above the substrate and then fixing h_s at the position of minimum energy.

The adsorbate sublattice has the lattice constant a_a, and the layer spacing d_a is equal to $\sqrt{3}a_a/2$. The height of the first adsorbate layer above the substrate, h_a, is determined in the same way as h_s. The IL model assumes that the overlayers are flat, and thus the energy of the sites along the layer will vary according to how far a site on the adsorbate sublattice is offset from the substrate. Each site on the first three layers of the adsorbate sublattice is therefore assigned an energy equal to the average value for that layer. If this precaution is not taken, the adatoms would initially occupy the low-energy sites in preference to high-energy sites.

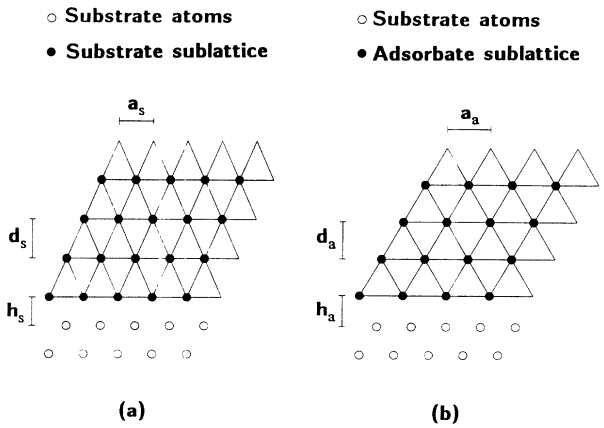

FIG. 1. (a) Substrate and (b) adsorbate sublattice above the substrate atoms as indicated. The IL model uses a superposition of the two sublattices.

The lattice used in the MC simulation is a superposition of the adsorbate sublattice and substrate sublattices. An adatom is introduced to the system by selecting a sublattice at random. The adatom is placed at the top of the crystal and moved down to the surface. The simulation then proceeds by the random selection of an adatom and a target site within the distance specified in Sec. II A to which the adatom may hop. A target site is available for occupation if it is not already occupied by another adatom. The energy of the adatom before and after the proposed hop is evaluated in order to determine the jump probability[18] and if the jump is successful the adatom is moved to its new location. This process is repeated a specified number of times before a new adatom is introduced into the system.

C. Potential-minimum model

The PM model has been described in detail in a previous publication (Faux *et al.*[20]) and so only a summary of the essential features will be presented here. It is assumed that atoms which vibrate about a mean position in a potential well may be represented as being fixed at a point at the well minimum. Only these minima may be occupied. The potential minima arise due to the interactions with the surrounding particles. Their positions therefore depend on the local environment and thus change as the simulation proceeds.

In the present case the locations of the potential minima are readily defined as the intersections of circles of radius a_a around adatoms and of radius a_{sa} around substrate atoms. Prior to the deposition of the first adatom, the available sites are the minima defined by the intersections of circles of radius a_{sa} around each substrate atom. These are labeled 1–3 in Fig. 2, which illustrates a portion of the total crystal. An adatom is deposited by selecting one of the available sites at random. In Fig. 2 an adatom has been added to site 2. A second adatom will now be able to occupy the extra sites defined by the intersections of circles of radius a_a around the adatom and a_{sa} around substrate atoms. These are labeled 4–7 in Fig 2. As the simulation proceeds, the majority of the available sites will arise due to the interaction between pairs of adatoms. As adatoms diffuse, some sites disappear and new sites are formed. It is possible that, due to the jump of one adatom, certain surrounding adatoms are no longer in a potential minimum. In this case the surrounding adatoms are moved immediately into the nearest available site. This crudely simulates the reconstruction which occurs after atomic motion. The simulation then proceeds in a manner similar to the IL model. An adatom and an available minimum are chosen at random and the energies of the initial and final states are calculated. The hop is then accepted or rejected according to the criterion described in Sec. II A.

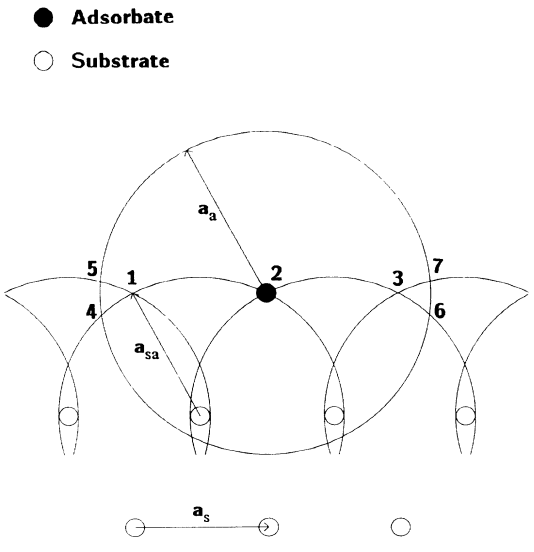

FIG. 2. Solid lines represent the loci of the potential minimum experienced by an adatom interacting with substrate (○) and adsorbate (●) atoms via a Lennard-Jones potential. The intersections of circles indicate positions of potential wells, and these wells may be occupied by adatoms. One adatom is shown in site 2. A second adatom may occupy sites 1–7, except site 2.

III. RESULTS

The growth process was monitored in two ways. First, outputs of the atomic positions were obtained at various stages during growth. This enables the growth mode to be examined as the simulation proceeds. Second, each layer of adatoms was monitored to assess whether the growth was in registry or incommensurate with the substrate. The precise monitoring technique is different for each model and is described in the appropriate subsection. Two temperatures were investigated, $kT/\varepsilon=0.06$ and 0.09. These correspond to about half and three-quarters of the melting point, respectively, and are the temperature parameters also chosen by Dodson and Taylor.[14] Kinetic effects are studied by changing the number of jumps made by the adatoms before a new adatom is deposited. The results obtained from each simulation are presented in the following subsections.

A. IL-model results

Simulations for the IL model were performed by depositing seven layers (280–350 atoms) at two different temperatures, $kT/\varepsilon=0.06$ and 0.09, for a range of lattice mismatches. The progresses of each run was monitored by counting the number of atoms on each layer of each sublattice as a function of the number of atoms deposited. A study of growth kinetics can be made by varying the the deposition rate, or, equivalently, by altering the number of attempted jumps per adatom which are made by the adatoms prior to the deposition of a new adatom. Note that the most convenient unit of time in the IL model is the attempted jump. One attempted jump is deemed to have occurred every time an adatom and a jump direction are chosen at random. At low temperatures an average of about 1% of all attempted jumps leads to a successful atomic jump, while at the higher temperature this success rate is 2%.

The program was checked by performing runs at the mismatch extremes of 2% and 8% with 400 attempted jumps per adatom between depositions and a temperature kT/ε of 0.06. The results are as expected: at 2% mismatch essentially all of the adatoms remain in registry with the substrate, while at 8% mismatch most adatoms occupy the adsorbate sublattice with only a few (about 5%) in the first deposited layer remaining on the substrate sublattice throughout the simulation.

The next set of runs were performed at 4% and 6% mismatch under the same conditions. The results at 4% mismatch are much the same as at 2%, with the exception that a noticeable fraction of the adatoms (about 15% in layers 6 and 7) occupies the adsorbate sublattice in the upper layers. The results at 6%, however, differ markedly from the results at 8% mismatch. Rather than occupying the adsorbate sublattice almost exclusively, deposited atoms switch from preferentially occupying the substrate sublattice to preferentially occupying the adsorbate sublattice during the course of the run. After three layers have been deposited, the second layer of the crystal has 70% of the adatoms on the substrate lattice, but with the deposition of only a few more adatoms an abrupt transition takes place, resulting in a distribution with about 60% of the adatoms on the adsorbate lattice. Similar results were observed for layers 4 and above, except that in the uppermost layers, where few adatoms have been deposited before the transition occurs, the adatoms tend to prefer the adsorbate lattice throughout the course of the run. Adatoms on the first layer remain primarily (70%) on the substrate lattice, suggesting that either the IL model, with its discrete sites, cannot accommodate a lattice transition when the overlayers are filled, or that the number of attempted jumps allowed imposes a kinetic limitation on the transition.

In order to study kinetic effects associated with changing the deposition rate, simulations were performed at 5% mismatch with 200, 1000, and 2000 attempted jumps per adatom between depositions at $kT/\varepsilon=0.06$. Figures 3(a) and 3(b) show the first-layer occupancy for both the adsorbate and substrate sublattices as a function of the number of adatoms deposited, for the runs at 200 and 2000 attempted jumps, respectively. The fractional occupancy was determined by recording the occupancy of the sublattices after each attempted jump (whether successful or not). The results displayed in Figs. 3(a) and 3(b) [and 4(a) and 4(b) as well] are obtained by averaging over an appropriate time period.

Results from the 200-jump simulation reveal adatoms occupying the substrate sublattice preferentially in all layers. Even among layers 6 and 7 the adatoms prefer the substrate sublattice nearly 4 to 1. Raising the number of attempted jumps to 1000 produces similar results in the lower layers, while noticeably more adatoms occupy adsorbate sites in the upper layers—the substrate to adsorbate occupancy ratio in layers 6 or 7 being reduced to nearly 2 to 1. When the number of attempted jumps is raised to 2000, the transition from the substrate to the adsorbate sublattice is more complete in the upper layers, with the substrate to adsorbate ratio reduced to 1 to 1. The additional jumps also allow the transition to propagate down to the first layer. Initially, atoms in the first layer occupy solely the substrate sites. Unlike previous runs, however, a shift towards the adsorbate lattice is observed in the first layer. The transition in layer 1 consists of two abrupt steps, one after approximately 120 atoms (three layers) have been deposited and a second after approximately 220 ($5\frac{1}{2}$ layers). By the end of the simulation, adatoms in layer 1 have shifted from 100% substrate site occupancy to 60% substrate and 40% adsorbate. Although the transition is far from complete, it is clear that increasing the number of attempted jumps per adatom (or, equivalently, by decreasing the deposition rate) allows the transition to propagate down to the first layer.

Although the number of attempted jumps could be increased even further to observe a more complete transition, it is costly to perform such long simulations. An alternative is to raise the system temperature so that a greater percentage of attempted jumps are successful. Accordingly, all of the simulations were repeated under

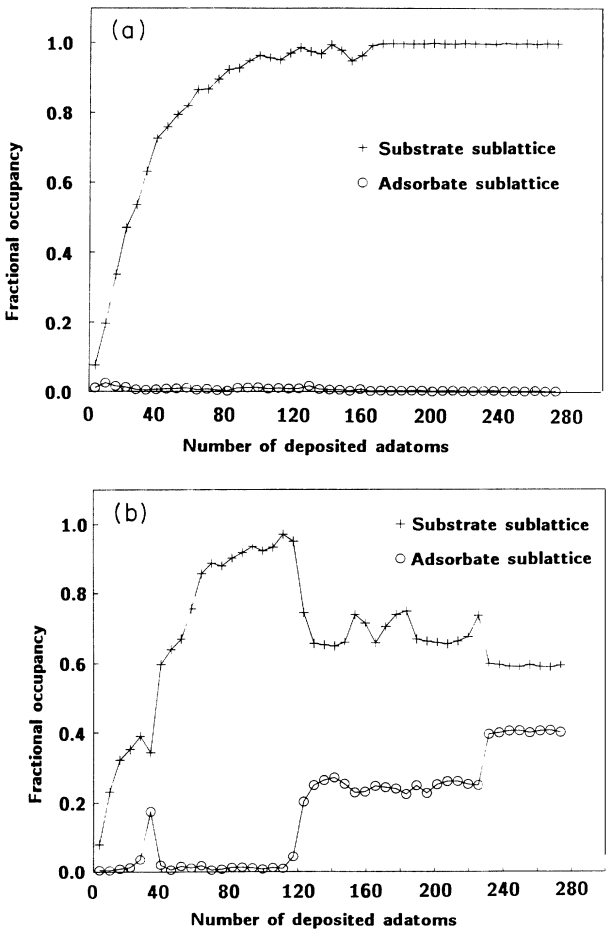

FIG. 3. Adsorbate sublattice occupancy (○) and substrate sublattice occupancy (+) plotted as a function of the number of adatoms deposited. These results are at 5% mismatch and $kT/\varepsilon=0.06$ at (a) 200 and (b) 2000 attempted jumps per adatom between depositions.

the same conditions at higher temperature.

The following results are at a temperature $kT/\varepsilon = 0.09$. The results for 2% mismatch and 400 attempted jumps resemble the results for 4% mismatch at the lower temperature. The results at 8% mismatch and 400 attempted jumps are similar to the results at the lower temperature, with most of the adatoms occupying the adsorbate sublattice and only a small fraction occupying the substrate sublattice. The results for 6% mismatch at the high temperature reveal that the substrate-to-adsorbate transition can be accomplished even on the first layer by raising the system temperature. Initially, the atoms are deposited on the substrate sublattice in the first layer, but from the time 60 atoms have been deposited to the time when 150 atoms have been added the adsorbate sublattice is preferred, resulting in a distribution that is 80% on the adsorbate sublattice and 20% on the substrate sublattice. This compares to 30% adsorbate and 70% substrate at the same stage at the lower temperature.

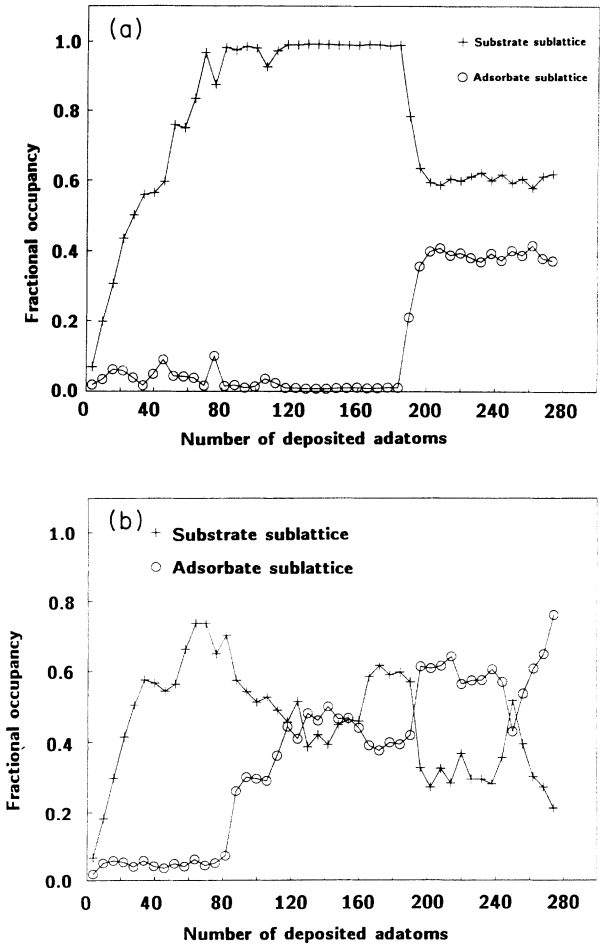

FIG. 4. Adsorbate sublattice occupancy (○) and substrate sublattice occupancy (+) plotted as a function of the number of adatoms deposited. These results are at 5% mismatch and $kT/\varepsilon = 0.09$ at (a) 200 and (b) 1000 attempted jumps per adatom between depositions.

A series of simulations at 5% mismatch with 200, 1000, and 2000 attempted jumps per atom were performed in order to investigate the effect of the deposition rate at the higher temperature. Figures 4(a) and 4(b) show the sublattice occupancy at 5% mismatch with 200 and 1000 attempted jumps per adatom, respectively, as a function of the number of adatoms deposited. For the 200-jump case, adatoms in the first layer initially occupy 100% substrate sites, but after the deposition of approximately 185 atoms ($4\frac{3}{4}$ layers) a transition occurs whereby about 40% of the first-layer atoms shift to the adsorbate lattice. Among the upper layers (6 and 7) the adsorbate sublattice is preferred, with adatoms occupying approximately 85% adsorbate sites. This is in contrast to the low-temperature results, which showed a first layer of 100% substrate occupancy and a substrate sublattice preference on all layers.

The high-temperature data also clearly show that the transition propagates from the upper layers to the lower layers. Table I shows the number of adatoms deposited when the transition from the substrate sublattice to the adsorbate sublattice begins on each layer for the 200-jump case. Also shown are the sublattice occupancies both before and after the transition. Although the transition in a layer occurs in abrupt steps, each step in a given layer is generally preceded by a step in the layers above it. The effect of increasing the number of attempted jumps to 1000 is twofold: First, the transition is more complete and, second, the transition begins after the addition of fewer adatoms. At 1000 attempted jumps, the transition in layer 1 begins after only 80 adatoms have been deposited and produces a first-layer occupancy which is 70% adsorbate and 30% substrate. Increasing the jump level to 2000 for the high-temperature system produces results similar to those at 1000 attempted jumps per adatom.

We now turn our attention to the growth mode. Snapshots of the simulation at various stages of growth reveal that the growth mode is van der Merwe (layer-by-layer) at 2% mismatch with small surface undulations in the topmost two layers or so. At 4% mismatch and higher, the tendency is for Volmer-Weber (island) growth with large clumps of deposited crystal forming on the substrate surface. Even after about six layers have been

TABLE I. Number of adatoms deposited when the transition occurs in a particular layer. The parameters for this run were 5% mismatch, $kT/\varepsilon = 0.09$, and 200 jumps/adatom between depositions. The percentage of adatoms on the substrate (S) and adsorbate (A) sublattices before and after the transition are indicated. These results demonstrate that the transition propagates from the upper layers towards the substrate surface.

Layer	No. of atoms deposited	S/A before (%)	S/A after (%)
4	160	60/30	45/55
3	175	90/10	50/50
2	180	100/0	55/45
1	185	100/0	60/40

deposited there is some substrate exposed, and the adsorbate appears as droplets on the surface. At 8% mismatch, although Volmer-Weber growth predominates, the islands are not as large as at the lesser mismatches and the islands coalesce to form a surface covering at an earlier stage than at the transitionary mismatches.

B. PM-model results

Analysis of results for the PM model differ from the IL model in two important ways. First, the unit of time was taken to be the successful jump per adatom, rather than the attempted jump per adatom. It is not possible to determine a realistic ratio between successful jumps and attempted jumps for the PM model as a single hop of an adatom is generally followed by a series of small reconstructing local hops as described in Sec. II C. Second, as there are no distinguishable sublattices, a different method for determining the degree of registry with the substrate is required. In the PM model the average nearest-neighbor distance for adatoms on each deposited layer is calculated, and this quantity is monitored continuously as the simulation proceeds. As before, snapshots of the atomic positions are made at regular intervals to assess the progress of the simulation.

Simulations were performed by the deposition of six layers (240–300 adatoms) at mismatches of 2%, 3%, 4%, 5%, and 8% at a temperature $kT/\varepsilon=0.09$. Typically, 5 jumps/adatom were made before the addition of the next adatom to the surface, except at 5% mismatch, where 10 jumps/adatom were made. At both 2% and 3% mismatch the adsorbate grows in registry with the substrate, as expected. The average nearest-neighbor atomic spacing in the first layer at 2%, 5%, and 8% is plotted in Fig. 5 as a function of the number of adatoms deposited. At 2% mismatch the initial atomic spacing appears to correspond to a_a rather than a_s. In fact, the calculation of the mean atomic spacing leads to an overestimate at the early stages of growth because, after a small number of adatoms have been deposited, there are very few adatoms with a nearest neighbor, and those that do possess a nearest neighbor tend to be separated by a distance a_a. Thus, this method of calculation does not take into account the many isolated adatoms present on the surface. After the first layer is full, the average lattice spacing is indeed a_s.

At 4% mismatch (not shown) the average nearest-neighbor spacing is roughly midway between a_s and a_a. At 8% mismatch, misfit growth is observed at all stages of growth, as illustrated in Fig. 5. At the intermediate mismatch of 5% a transition is observed from registered to misfit growth. The average lattice spacing is plotted in Fig. 5 and shows a fall at the early stages of growth (up to two layers or 80 adatoms deposited) similar to that for the 2% case. After about two to three layers have been deposited (80–120 adatoms), however, the average atomic spacing levels off and then rises to the value a_a. The average spacing between nearest-neighbor adatoms on the higher layers is always larger than that in the first layer, and indicates that the transition propagates downwards from the crystal surface.

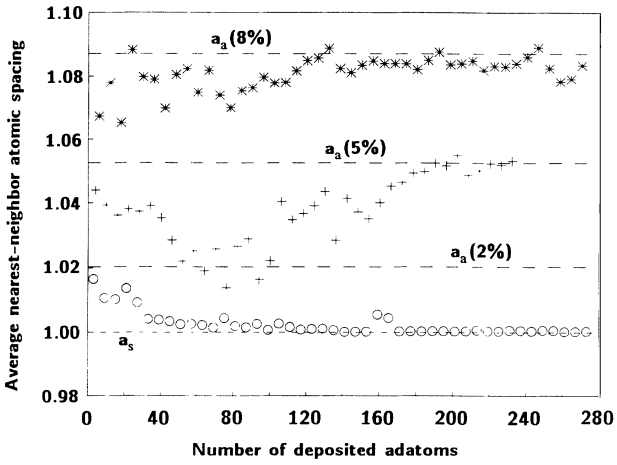

FIG. 5. Mean spacing between nearest-neighbor adatoms on the first layer is plotted as a function of the number of adatoms deposited for the PM model. These results are for $kT/\varepsilon=0.09$ at lattice mismatches of 2% (○), 5% (+) and 8% (∗).

Additional runs were performed at $kT/\varepsilon=0.06$ with the same number of jumps per adatom as before. Similar results were obtained in this case. This is not surprising, as the primary effect of raising the temperature in the IL model was to increase the jump acceptance rate. Raising the number of jumps per adatom to 20 in the present case also had little effect on the results, indicating that satisfactory equilibrium has been achieved. Reducing the jump rate to 1 jump/adatom at 5% mismatch, however,

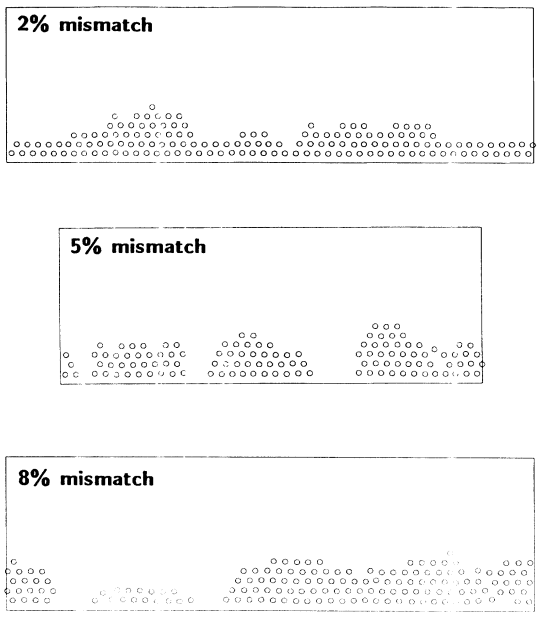

FIG. 6. Positions of the adatoms after three layers have been deposited at $kT/\varepsilon=0.09$ for the PM model. Results are shown at 2%, 5%, and 8% mismatch.

had the effect of inhibiting the transition. The average nearest-neighbor spacing in the first layer was about halfway between a_s and a_a, and the overall results were similar to those at the 4% mismatch previously.

The simulations using the PM model clearly illustrate the change in growth mode as the mismatch increases. Figure 6 shows the surface after three layers have been deposited at mismatches at 2%, 5%, and 8%. At 2% mismatch, van der Merwe growth is observed with small surface undulations. At 5% mismatch the Volmer-Weber–growth mechanism is most clearly observed, and at 8% mismatch, although Volmer-Weber growth predominates, its effect is not so extreme. Once again, these observations are similar to those from the IL model and illustrate the importance of strain in determining the growth mode.

IV. DISCUSSION

Similar results are obtained from both the IL and PM models despite a number of important differences between them. For instance, the PM model allows a greater freedom of movement because there are roughly 14 sites which may be occupied per adatom, compared to two in the IL model. This may inhibit the transitions in the IL model. The majority of hops in the PM model are, however, small rearrangement jumps. Longer jumps are made by the adatoms at the surface, which are obviously more mobile. The placement of adatoms directly in potentials wells in the PM model means that adatoms do not have to make many jumps before locating a well, as in continuous-space simulations.

The process of evaporation is ignored in the PM model for the results presented here, although it would be straightforward to incorporate this effect into the model. In the IL model, however, evaporation can occur quite naturally during the course of the simulation. An adatom may jump from the surface to sites away from the surface and therefore escape from the crystal. Even so, evaporation rates are very small during the simulations presented here. A further difference between the models concerns the sites occupied by the first layer of adatoms in the case of incommensurate growth. In the IL model the first adsorbate layer is flat because the adatoms are confined to the sites of the adsorbate sublattice. In the PM model, however, the first layer is slightly undulated. This is because adatoms directly above substrate atoms will be further away from the substrate surface than an adatom in a site equidistant between two substrate atoms. This curvature is transferred to the upper layers, which are therefore undulated in the same manner. The PM model thus exaggerates the effect of a perturbation in the surface layer by transferring its effect to upper layers, while the IL model ignores this perturbation completely. No such curvature in the adsorbed layers seems to appear in the continuous-space MC results of Dodson and Taylor,[14] but it is clearly present in their molecular-dynamics work.[15] It is satisfying that both the IL and PM models produce similar results.

Both models may be extended to three dimension with spherical potentials. In the case of the PM model, the potential minima can be defined as the intersection of three spheres. Modifications to the model would be required if more complicated potentials are to be implemented, as the minima are less easily defined. The potentials devised by Stillinger and Weber[13] and by Tersoff[21] for silicon are, however, short ranged, and so the minimum in potential due to the nearest neighbors would be the true local energy minimum for these potentials. Work is underway to develop a modified version of the PM model incorporating these potentials.

The major advantage of discrete-space computer models is that they are inherently faster than continuous-space techniques. For the PM model, typically 200 adatoms may be deposited in 10 h on a Digital Equipment Corporation microVAX II computer using 10 jumps/adatom. The IL model consumes a similar amount of time. Direct comparisons are difficult, but this appears to be a factor of 2–5 faster than previous continuous-space work. Further speedups have been obtained in the IL model by employing a technique equivalent to using a vacancy-diffusion scheme in lattice-gas systems. The majority of adatoms are unable to move because neighboring sites are occupied by adatoms, and so it is beneficial to first determine the possible vacant target sites for a hop and to consider moving only those adatoms which may jump to these. This makes a further factor of about 3 improvement to the times reported here. Further improvements may be made by employing a random-walk "zone" annealing scheme.[22]

V. CONCLUSIONS

Both the IL and PM models yield similar results, differing only in detail. Registered growth is observed at small mismatches ($\lesssim 4\%$) and incommensurate growth is observed at large mismatches ($\gtrsim 6\%$) during simulations for which a total of six to seven layers were deposited. This is in general agreement with Taylor and Dodson,[15,16] although we observe broadly similar results at both temperatures, while Taylor and Dodson observe incommensurate growth at 3–4 % mismatch at the higher temperature. At 5% mismatch our simulations show a transition in which the adatoms initially grow in registry with the substrate until a few layers have been deposited, and then a switch is observed to incommensurate growth. The transition commences in the upper layers and propagates down toward the first deposited layer. No such transition is reported by Taylor and Dodson.

Both models reveal that van der Merwe growth predominates at 2% mismatch, while Volmer-Weber growth is preferred at larger mismatches. The strain clearly influences the growth mode, and these conclusions are in agreement with Berger *et al.*,[23] who also suggest that Volmer-Weber growth should predominate at mismatches greater than about 2%. We also find, however, that the tendency for island growth is greatest at the transitionary mismatches and is slightly reduced at the larger mismatches, where the growth is incommensurate with the substrate at a very early stage. Interestingly, Berger *et al.* observe a transition in the surface lattice

constant with temperature. Studies of kinetic effects in the present IL simulations show that the surface lattice constant (or the fraction of adatoms on the adsorbate sublattice) increases with temperature, in qualitative agreement with Berger *et al.*

ACKNOWLEDGMENTS

One of us (D.A.F.) would like to thank the United Kingdom Science and Engineering Research Council for partial support when most of this work was performed.

*Present address: Department of Physics, University of Chicago, Chicago, IL 60637.

[1] *Epitaxial Growth,* edited by J. W. Matthews (Academic, New York, 1975).

[2] L. L. Chang, J. Vac. Sci. Technol. B **1**, 120 (1983).

[3] A. Y. Cho, Thin Solid Films **100**, 291 (1983).

[4] G. C. Osbourn, J. Vac. Sci. Technol. **21**, 469 (1982); Phys. Rev. B **27**, 5126 (1983); J. Vac. Sci. Technol. A **3**, 826 (1985).

[5] E. P. O'Reilly, Semicond. Sci. Technol. **4**, 121 (1989).

[6] H. Muller-Krumbhaar, in *Monte Carlo Methods in Statistical Physics,* edited by K. Binder (Springer, New York, 1979).

[7] J. Singh and A. Madhukar, J. Vac. Sci. Technol. **20**, 716 (1982); **21**, 562 (1982); J. Vac. Sci. Technol. B **1**, 345 (1983).

[8] A. Madhukar, Surf. Sci. **132**, 344 (1983).

[9] S. Clarke and D. D. Vvedensky, Phys. Rev. Lett. **58**, 2235 (1987).

[10] S. Clarke and D. D. Vvedensky, J. Appl. Phys. **63**, 2272 (1988).

[11] M. Schneider, A. Rahman, and I. K. Schuller, Phys. Rev. Lett. **55**, 604 (1985).

[12] M. Schneider, I. K. Schuller, and A. Rahman, Phys. Rev. B **36**, 1340 (1987).

[13] F. H. Stillinger and T. A. Weber, Phys. Rev. B **31**, 5262 (1985).

[14] B. W. Dodson and P. A. Taylor, Phys. Rev. B **34**, 2112 (1986).

[15] P. A. Taylor and B. W. Dodson, Phys. Rev. B **36**, 1355 (1987).

[16] A. Kobayashi and S. Das Sarma, Phys. Rev. B **37**, 1039 (1988).

[17] S. Das Sarma, S. M. Paik, K. E. Khor, and A. Kobayashi, J. Vac. Sci. Technol B **5**, 1179 (1987).

[18] K. Binder, in *Monte Carlo Methods in Statistical Physics,* edited by K. Binder (Springer, New York, 1979).

[19] H. C. Kang and W. H. Weinberg, J. Chem. Phys. **90**, 2824 (1989).

[20] D. A. Faux, C. K. Hall, J. Bernholc, Mol. Sim. (to be published).

[21] J. Tersoff, Phys. Rev. Lett. **56**, 632 (1986).

[22] C. L. Carson, J. Bernholc, D. A. Faux, and C. K. Hall, Appl. Phys. Lett. **56**, 1971 (1990).

[23] P. R. Berger K. Chang, P. Bhattacharya, J. Singh, and K. K. Bajaj, Appl. Phys. Lett. **53**, 684 (1988).